CHAPTER V

RESULTS AND DISCUSSION

The effect of thermal curing temperature (300-350°C), different atmosphere and concentration of zinc oxide nanoparticles in polyimide (PI) films on photoluminescence properties were studied. Crystal structure and dispersion of ZnO nanoparticles in PI films were also investigated. In addition, thermal properties of the films which were changed due to the presence of ZnO were studied.

5.1 Identified crystal structure of ZnO

Note that, there were two ways of preparing hybrid films. First, adding ZnO nanoparticles into PAA solution directly. Then PAA was imidized and ZnO in PI film was obtained and was defined as ZnO/PI. The other method was adding zinc nitrate hexahydrate into PAA solution. Zinc nitrate hexahydrate in this solution was then converted to ZnO while PAA was imidized to be PI and the material was defined as Zn nitrate/PI. Crystal structure of ZnO nanoparticles in PI films was investigated by X-ray diffraction (XRD) technique.

The X-ray diffraction (XRD) patterns of ZnO in PI films were shown in figure 5.1. The XRD peaks corresponding to the basal reflection of ZnO was an indicative that crystal structure of ZnO were presented in the film [*10*]. The detail of plane reflection of crystal structure of ZnO was shown in appendix B. The XRD patterns of 35.1 mol% ZnO/PI showed wurtzite ZnO hexagonal phase which was consistent with the standard values for bulk ZnO. In addition, the position of the first three XRD peaks of both 3.3 mol% ZnO/PI and 666.6 mol% Zn nitrate/PI was clearly observed; therefore, crystal structure of ZnO were the wurtzite ZnO hexagonal phase.

35.1 mol% ZnO/PI showed the clearest peak indicating the presence of ZnO crystal in PI films while the XRD peaks of 3.3 mol% ZnO/PI showed smaller and broader peaks due to lower concentration than that film. However, 35.1 mol% ZnO/PI

film exhibited sharper peak than 666.6 mol% Zn nitrate/PI film. It could be due to an imperfect crystal structure and small size of ZnO in Zn nitrate/PI film. From Scherrer's formula equation, ZnO nanoparticle's size of 35.1 mol% ZnO/PI and 666.6 mol% Zn nitrate/PI was 13.5 and 5 nm, respectively (as shown in appendix C).

Furthermore, 666.6 mol% Zn nitrate/PI showed broad peaks and low intensity. Therefore zinc nitrate hexahydrate could be converted to ZnO particles by thermal decomposition. However, 117.6 mol% Zn nitrate/PI did not show the XRD peaks. It could be due to small particles size, imperfect crystal structure and too little amount of ZnO in PI that was under the limitation of diffractometer. This result was consistent with Sawada and Ando [*19*] and Chiang and Whang [*20*].

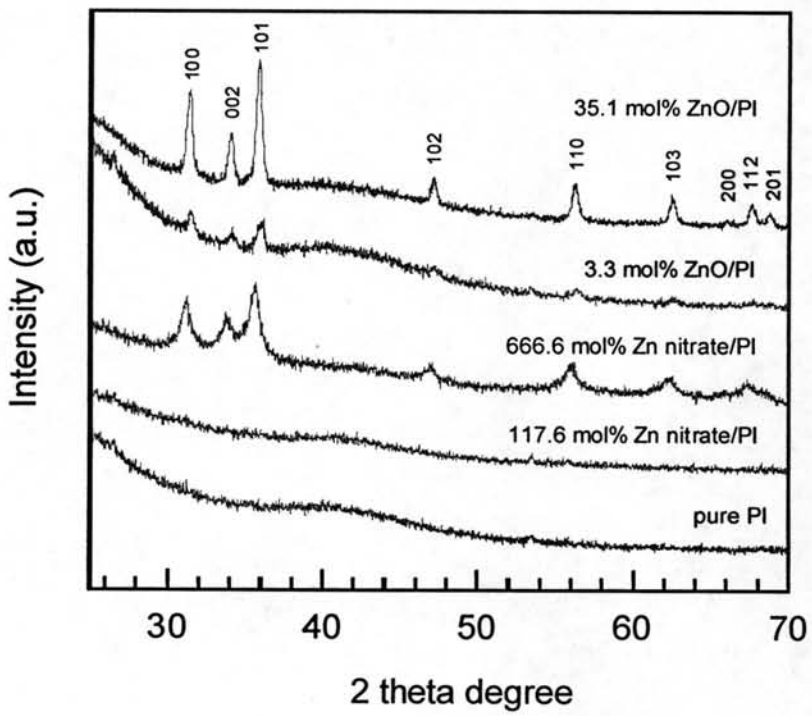

Figure 5.1 XRD patterns of pure PI, PI with ZnO nanoparticles from thermal-decomposition of zinc nitrate hexahydrate and ZnO nanoparticles directly added into PI.

5.2 Imidization of 6FDA/TFDB poly(amic acid) films

Figure 5.2 shows the IR spectra of poly(amic acid) (PAA) and pure polyimide (PI). From the figure, the characteristic peaks for PAA at 1726 cm^{-1} for carbonyl stretching vibration (C=O) in carboxylic acid group (COOH), 1680 cm^{-1} for carbonyl group (C=O) in CONH and at 1537 cm^{-1} for C-NH stretch band, were presented. Then imidization of PAA films at 300°C curing temperature, the polyimide (PI) ring-closing reaction led to a chain growth as indicated by the disappearance of those characteristic PAA bands. An identification of the PI formation was performed by observing the imide bands at 1785 and 1724 cm^{-1} for carbonyl stretching vibrations and 1364 cm^{-1} for stretching vibrations of C-N. This result was consistent with Hsu et al's [*21*]. In addition, the imide bands at 1785, 1725 and 1365 cm^{-1} were observed in Zn nitrate/PI films as shown in figure 5.3. Decrement of the characteristic imide peaks at 1725 cm^{-1} of Zn nitrate/PI films at 74.1 mol% and higher concentration compare to that of other hybrid films was observed.

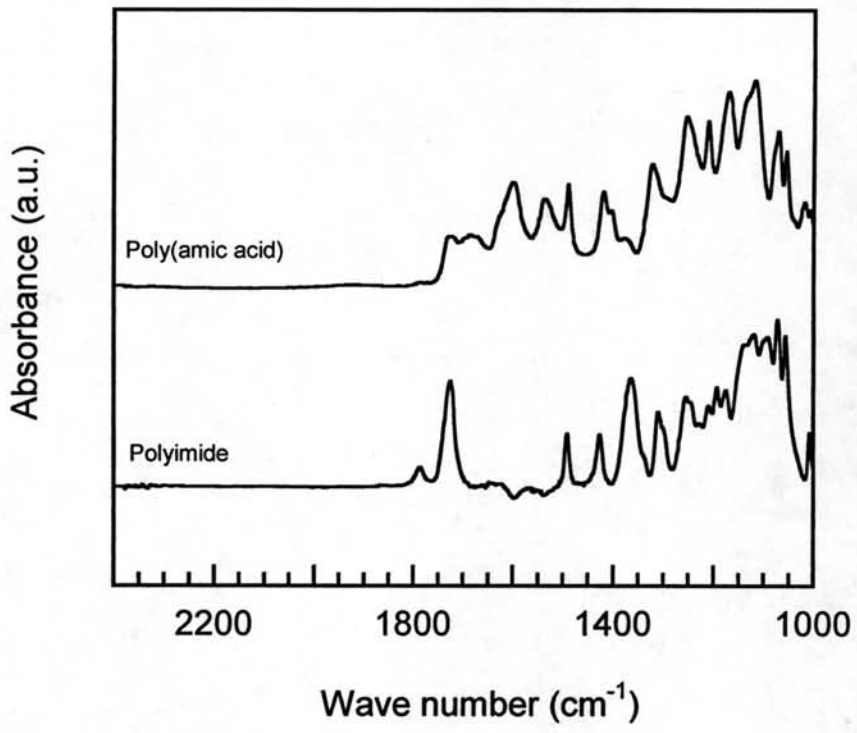

Figure 5.2 ATR-FTIR spectra of 6FDA/TFDB poly(amic acid) films and polyimide films prepared at 70°C for 1 hour and 300 °C for 1 hour under nitrogen atmosphere.

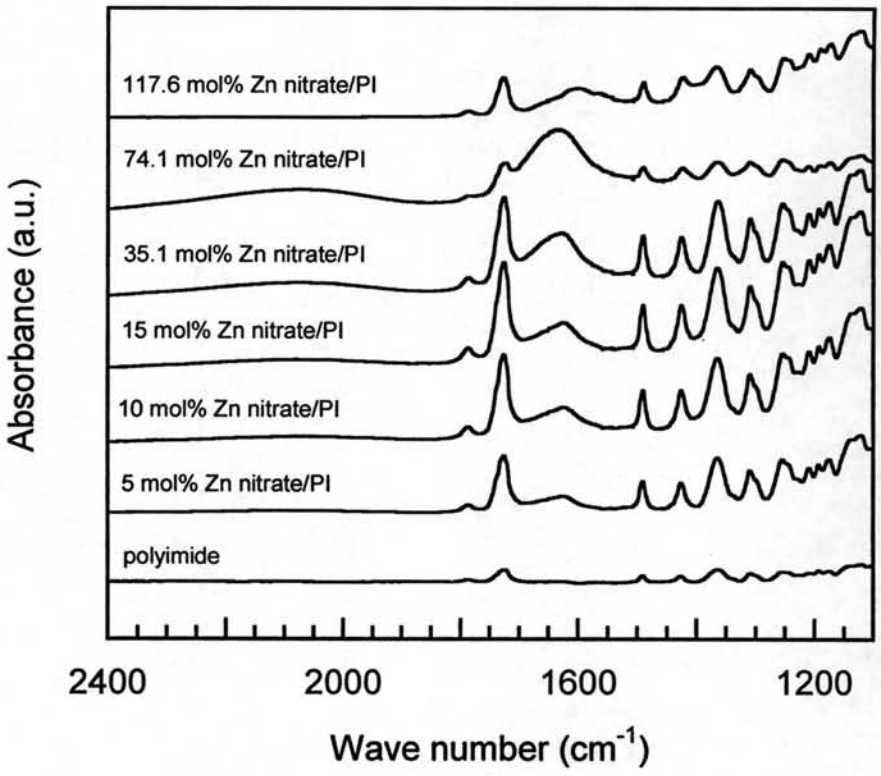

Figure 5.3 ATR-FTIR spectra wave number between 600-2000 cm^{-1} of pure polyimide and Zn nitrate/PI films for all concentration prepared at 300°C under nitrogen atmosphere.

5.3 Thermal properties

5.3.1 Glass transition temperature

Glass transition temperature (T_g) of pure PI and hybrid films, ZnO/PI and Zn nitrate/PI, were characterized by differential scanning calorimeter (DSC) under nitrogen atmosphere at heating rate 20°C/minute, temperature range from 50 to 480°C. The result shown in figure 5.4 and 5.5 was reheated sample's data. Figure 5.4 showed DSC thermograph of Zn nitrate/PI in which the T_g of these samples was not observable. It could be cause by the oxidation of ZnO during imidization of Zn nitrate/PI films. The brittleness of film was observed and it could be due to the formation of ZnO from Zn nitrate which affected the mobility of polymer chain. Thus, T_g of Zn nitrate/PI was not observed.

Figure 5.5 showed T_g and DSC thermograph of pure PI and ZnO/PI. The T_g of hybrid films of 0.6 and 3.3 mol% ZnO/PI remained the same as that of pure PI which was 336°C. This result was consistent with Chae and Kim's [*22*]. The T_g of 35.1, 74.1 and 117.6 mol% ZnO/PI slightly increased to 337.30, 338.87 and 339.44°C, respectively when compared with that of pure PI. This result was consistent with Hsu et al's [*21*] and Chae and Kim's [*22*]. Adding solid filler into polymer would reduce the mobility of polymer chain. Consequently, the increment in T_g value occured [*23*]. There were two major contributions to the mobility of polymer chains in composites; i.e., tethering and chain confinement [*22,23*]. The chain tethering was an attractive force between filler surfaces and polymer chains. However, the chain confinement occurred when the mobility of polymer chains was obstructed by fillers. Therefore T_g value at 35.1 mol% and higher concentration in ZnO/PI which slightly increased could caused by chain confinement due to little attractive force between surface of ZnO and polymer chains. This result was consistent with Chae and Kim's [*22*].

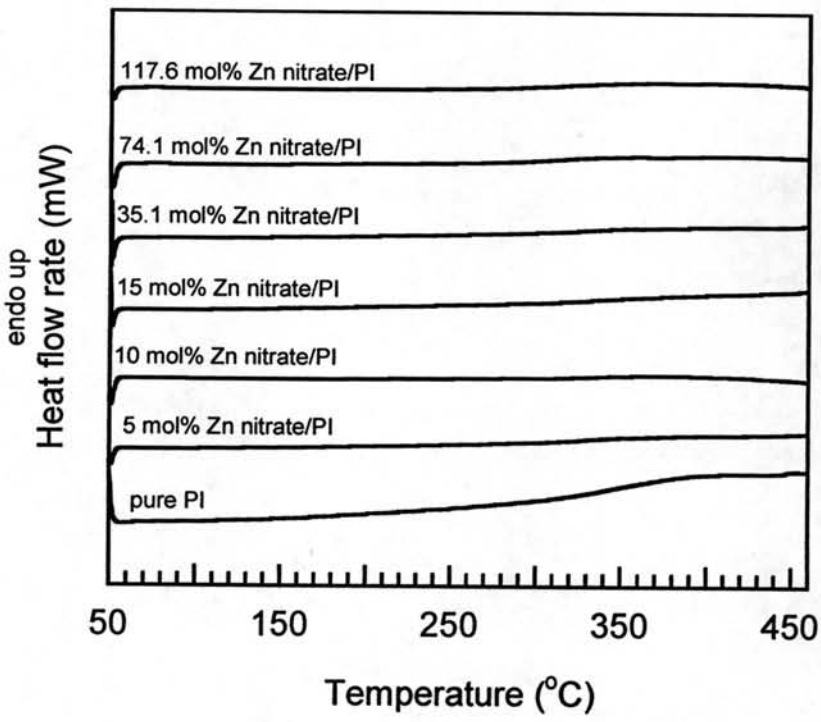

Figure 5.4 DSC heating scan thermograms of PI containing ZnO nanoparticles from thermal decomposition of zinc nitrate hexahydrate.

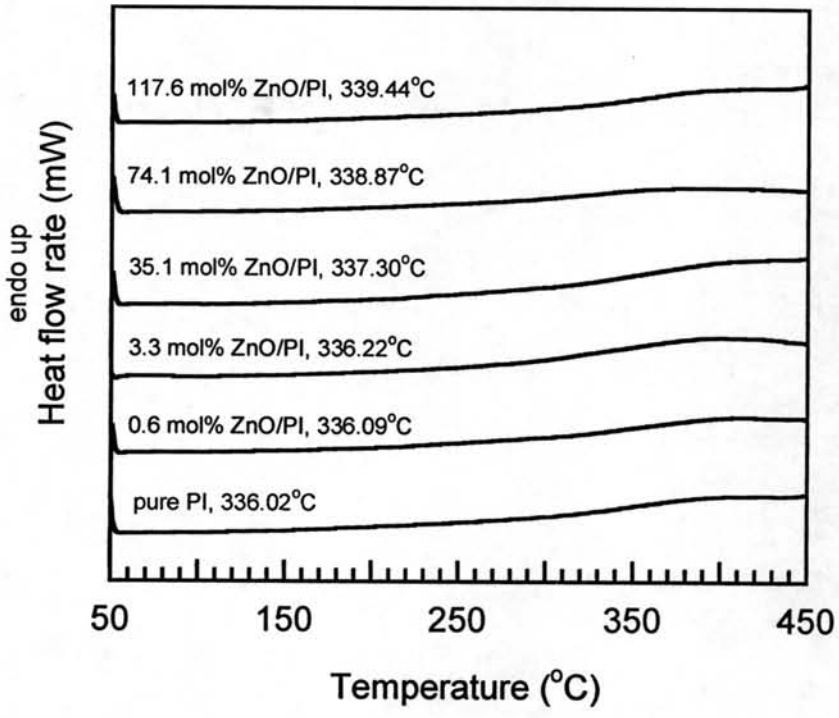

Figure5.5 DSC heating scan thermograms of PI containing directly added ZnO nanoparticles.

5.3.2 Degradation temperature

The presence of ZnO in PI films affected their degradation temperature (T_d). Thermal degradation temperature, which was defined as the temperature of material at 5 wt% loss, of Zn nitrate/PI films and ZnO/PI films were characterized by thermogravimetric analyzer at heating rate 20°C/minute under nitrogen atmosphere. It has been observed that T_d of Zn nitrate/PI was lower than that of ZnO/PI. Figure 5.6 showed a thermogravimetric profile of Zn nitrate/PI films. As shown in table 5.1, the degradation temperature of pure PI film was 555°C. Adding only 5 mol% of zinc nitrate into PI, the degradation temperature decreased 17°C compared with that of pure PI. Then adding more amount of Zn nitrate/PI from 5 to 117.6 mol% T_d has dramatically decreased from 17 to 204 °C compare with that of pure PI films as shown in table 5.1.

Figure 5.7 showed a thermogravimetric profile of ZnO/PI films. The degradation temperature of these hybrid films slightly decreased when adding ZnO nanoparticles directly into the films as shown in table 5.1. Adding 0.6 mol% of ZnO into PI, the degradation temperature decreased only 20°C when compare with that of pure PI. Adding more amount of ZnO/PI from 0.6 to 117.6 mol%, T_d gradually decreased in range of 20 to 50°C compared with that of pure PI films as shown in table 5.1. Furthermore, ZnO/PI and Zn nitrate/PI at same concentration, 35.1 mol% showed different thermogravimetric profiles. The T_d of ZnO/PI was slightly decreased by 35°C while that of Zn nitrate/PI was obviously decreased by 132°C. Therefore ZnO/PI film was more thermal stable than the Zn nitrate/PI film.

Distinction between T_d of ZnO/PI and that of Zn nitrate/PI film could be a consequence of the origin of ZnO nanoparticles. Because metallic compounds added into PI films induced oxidation and degraded polyimide [*19,20*], it decreased the T_d of Zn nitrate/PI film dramatically. This result was consistent with Hsu et al [*21*] and Chiang and Whang [*20*].

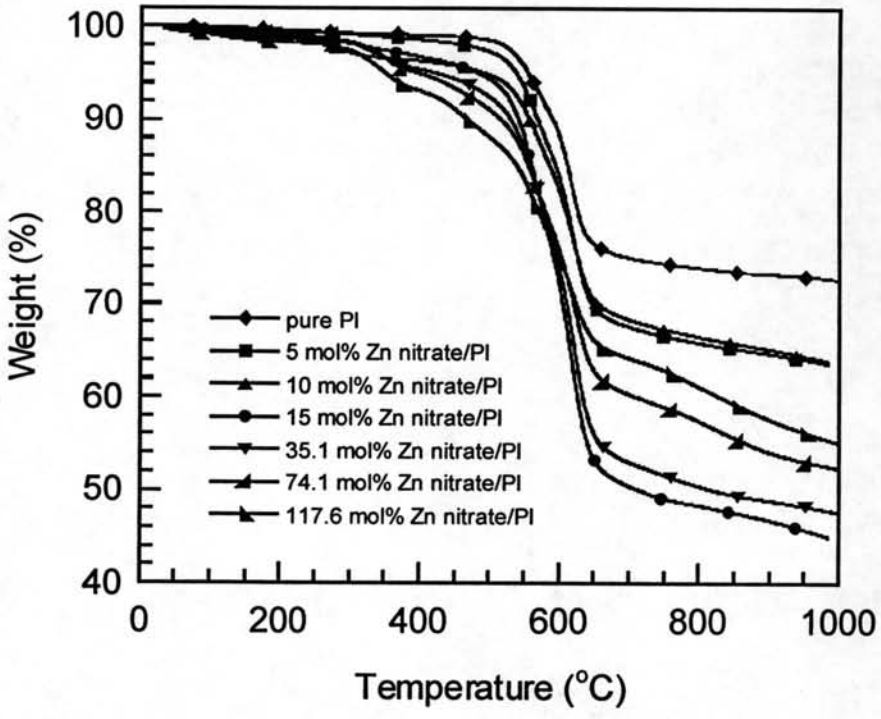

Figure 5.6 Thermogravimetric profiles of PI containing ZnO nanoparticles from thermal decomposition of zinc nitrate hexahydrate.

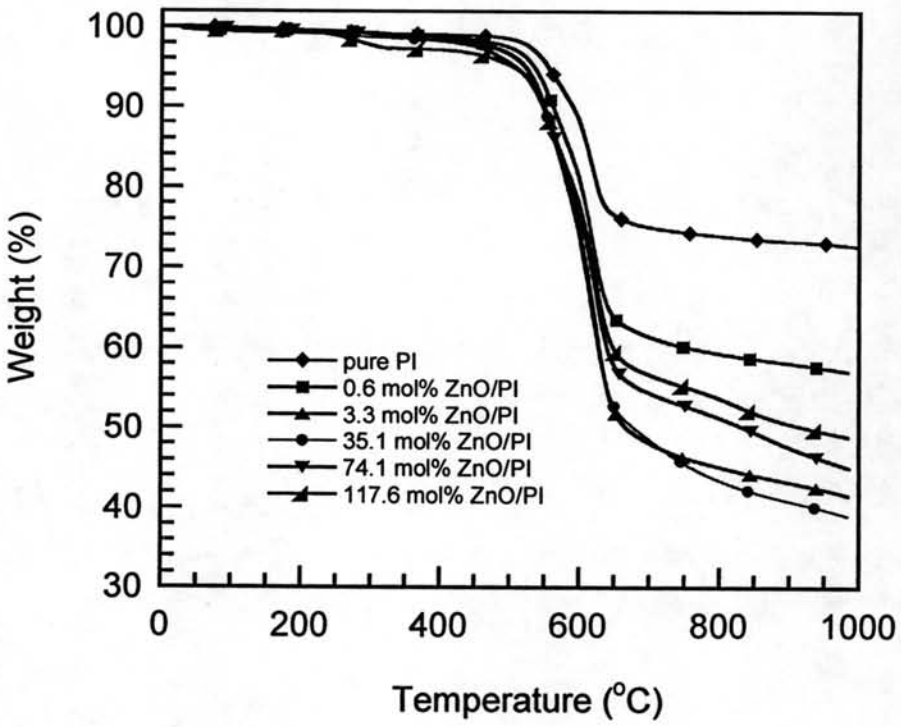

Figure 5.7 Thermogravimetric profiles of PI containing ZnO nanoparticles.

Table 5.1 The degradation temperature of pure PI, ZnO/PI and Zn nitrate/PI.

ZnO content (mol%)	Zn nitrate/PI		ZnO/PI	
	T_d (°C)	ΔT_d (°C)	T_d (°C)	ΔT_d (°C)
Pure PI	555	-	555	-
0.6	-	-	535	-20
3.3	-	-	523	-32
5	538	-17	-	-
10	494	-61	-	-
15	484	-71	-	-
35.1	423	-132	520	-35
74.1	399	-156	508	-47
117.6	351	-204	505	-50

T_d was defined as T of material at 5 wt% loss.

$\Delta T_d = T_d - T_d$ (pure PI)

5.4 Optical properties

Figure 5.8 showed the optical absorbance and photoluminescence spectra at room temperature as a function of wavelength of pure PI film and 0.6 mol% ZnO/PI that was imidized at 300°C under nitrogen atmosphere. The exciton absorption peak of pure PI film and hybrid film at 316 and 314 nm was observed respectively. The absorption in the range of 314 - 400 nm was observed for both pure PI and hybrid films. Above 400 nm, the absorption was quenched in visible region for both films. The absorption could be attributed to the transition from the ground state to an excited state in a few defect related to a deep state. However, the exciton absorption peak of a hybrid film was shown at shorter wavelength (314 nm) than that of the pure PI film (316 nm). This may be attributed from the presence of ZnO nanoparticles. Furthermore, the exciton absorption peak of hybrid film was substantially blue shifted

compared with that of bulk ZnO (~373 nm) due to the strong confinement effect. This result was consistent with Guo and Yang's [*24*].

The pure PI was emitted at 474 nm which were excited at 334 nm and hybrid film was emitted at 475 nm which were excited at 338 nm. The first-round emission spectra was obtained by fixing excitation wavelength. The obtained emission peak was then used to obtain excitation spectra. Next, the excitation-emission scans were performed back and forth until certain emission and excitation peaks were obtained at the same wavelength as the previous scan. However, adding only 0.6 mol% ZnO enhanced intensity of emission peak by 2.2 times when compared to that of pure PI. In this study, the thickness of all films was about 10 μm and other parameters were the same. Therefore, intensity enhancement of emission peak of 0.6 mol% ZnO was due to high quantum efficiency.

5.4.1 Effect of curing temperature on photoluminescence

The optical absorbance and photoluminescence spectra at room temperature of PI films containing 35.1 mol% ZnO/PI at different curing temperature were shown in figure 5.9. The exciton absorption peak of ZnO/PI films of all curing temperature were shown at 305 nm. The absorption spectra of all films in the range of 305 – 410 nm were observed. Above 410 nm, the absorption was then quenched in the visible region. The emission peak of all films was shown at 461 nm for both 300 and 325°C curing temperature and was slightly red shifted to 469 nm for film cured at 350°C. The light emission intensity slightly increased when increasing curing temperature of the hybrid films. Therefore, the curing temperature slightly affected the light emission intensity. The effect of curing temperature of other ZnO concentrations on photoluminescence exhibited the same trend and was shown in appendix D. Due to slightly effect of curing temperature on light emission intensity; curing temperature at 300°C was chosen to explore other effects on photoluminescence.

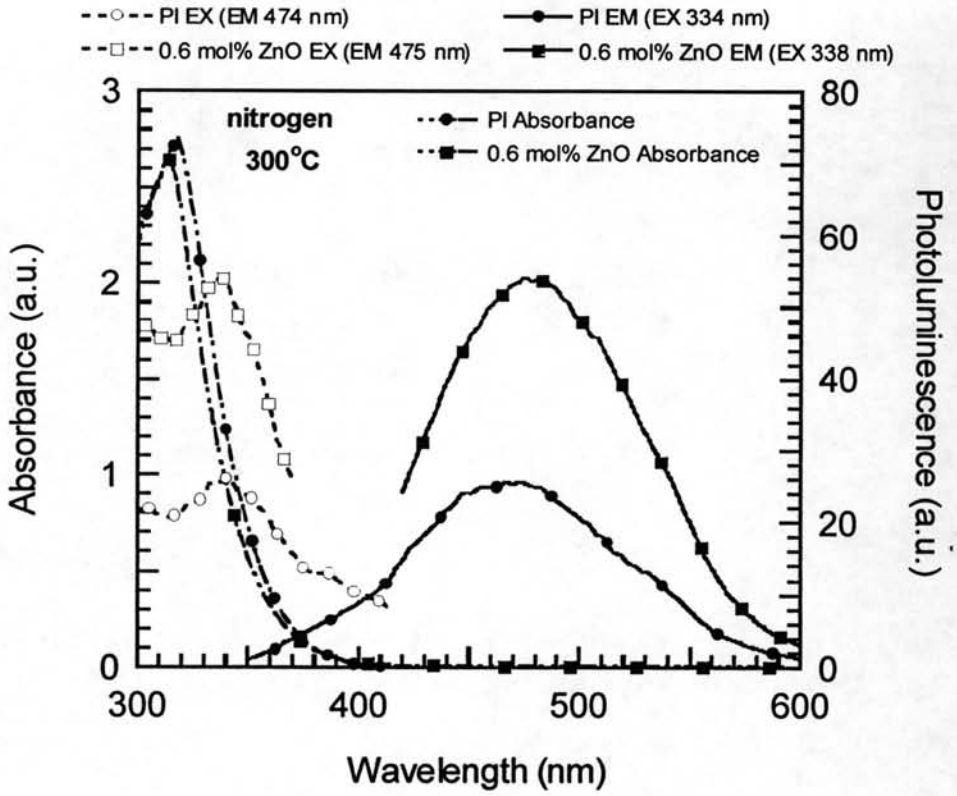

Figure 5.8 Photoluminescence of pure PI and 0.6 mol% ZnO/PI under nitrogen atmosphere at 300°C curing temperature.

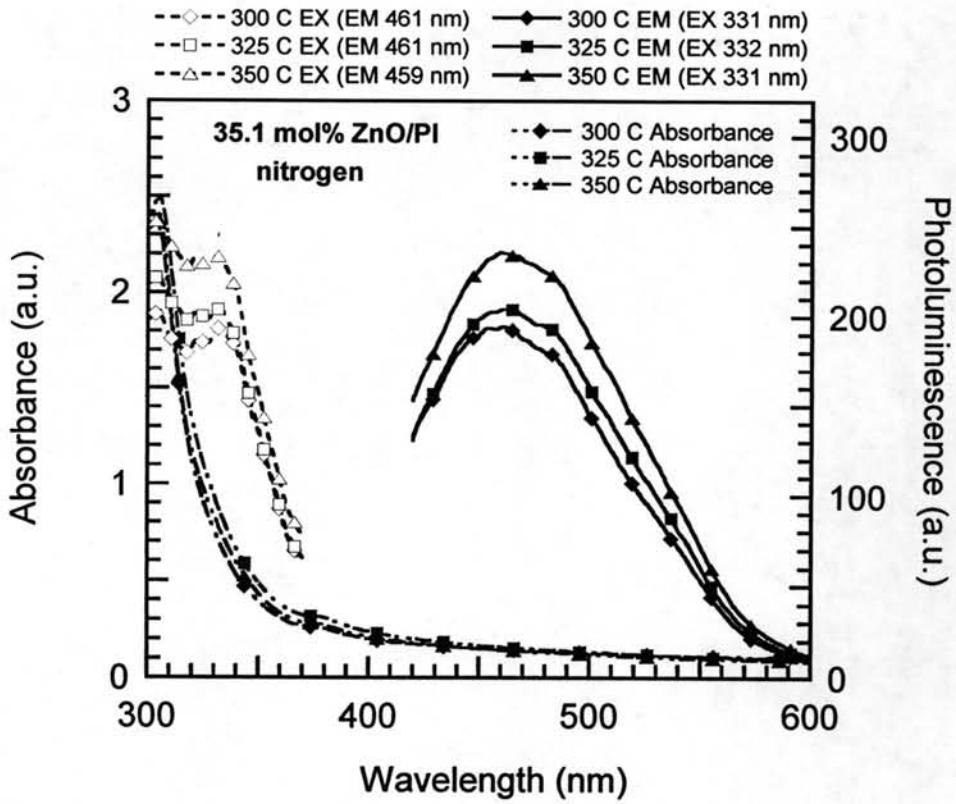

Figure 5.9 Effect of curing temperature on photoluminescence of 35.1 mol% ZnO/PI under nitrogen atmosphere.

5.4.2 Effect of curing atmosphere on photoluminescence

The effect of curing atmosphere on photoluminescence between nitrogen and argon had been studied. Figure 5.10 showed the absorbance and photoluminescence at room temperature of 35.1 mol% ZnO/PI films. The films were imidized at 300°C under both nitrogen and argon atmosphere. The exciton absorption peak of the films cured under nitrogen and argon atmosphere were observed at 302 and 307 nm, respectively. The absorbance spectra of both nitrogen and argon atmosphere were observed in the range of 300 – 400 nm. Above 400 nm, the absorption was then quenched in the visible region. The light emission of the film prepared under nitrogen atmosphere showed emission peak at 461 nm and excitation peak at 331 nm. Light emission of the films prepared under argon atmosphere showed

emission peak at 457 nm and excitation peak at 332 nm. The light emission of the film prepared under nitrogen was slightly red shifted and exhibited 2.4 times higher intensity than that prepared under argon atmosphere. Roy et al [*15*] showed that ZnO synthesized under nitrogen atmosphere emitted higher intensity of green light that those done under argon atmosphere. The effect of curing under nitrogen and argon atmosphere at any ZnO concentrations was shown in appendix E and exhibited similar trends as these films.

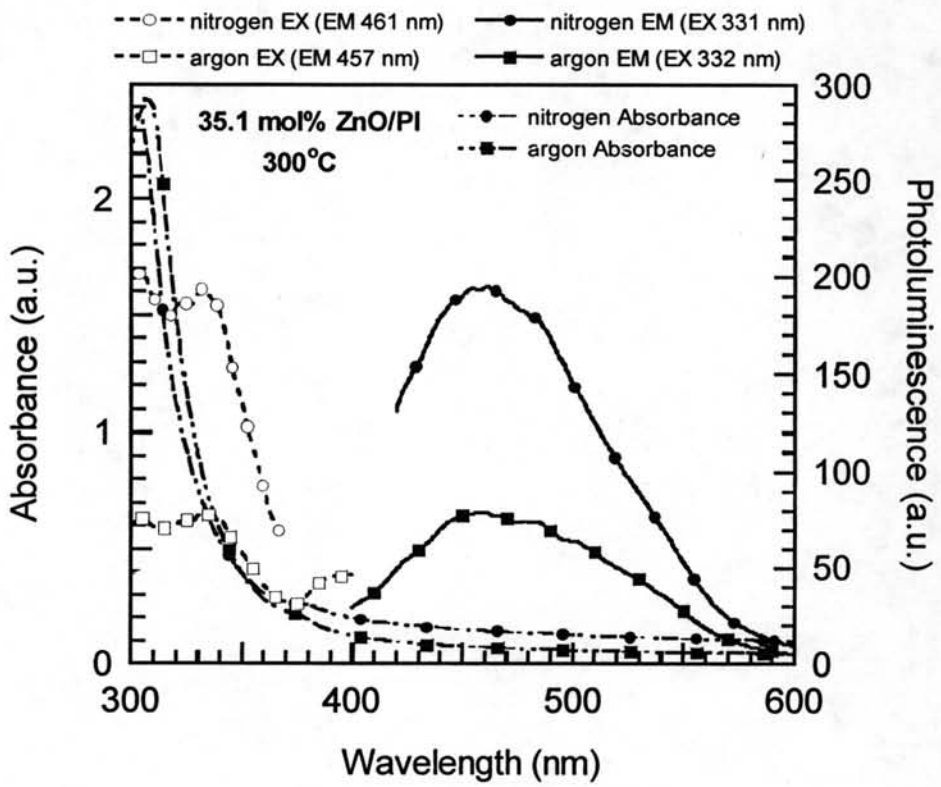

Figure 5.10 Effect of curing atmosphere on photoluminescence of 35.1 mol% ZnO/PI at 300°C curing temperature.

5.4.3 Effect of ZnO concentrations on photoluminescence

In this part, the effect of ZnO concentration on photoluminescence and absorbance was studied. The existence of ZnO in PI films enhanced the light emission. Figure 5.11 represented the effect of ZnO/PI concentration on the absorbance spectrum. The films were imidized at 300°C under nitrogen atmosphere. The increase in ZnO nanoparticle's concentration in the films from 0.6-117.6 mol%, the exciton absorption peak dramatically blue shifted from 318 to 295 nm and intensity decreased. However, the absorption peaks of the films prepared under argon atmosphere were random (appendix F). It was due to broad distribution of aggregation of ZnO nanoparticles in PI film which was confirmed by TEM image (Fig 5.17). The absorption spectra of all samples exhibited in the range of 300 – 370 nm. Above 370 nm, the absorbance of pure PI, 0.6 and 3.3 mol% ZnO/PI films was quenched in a visible region. However, the increase in absorbance intensity in visible region (above 370 nm) can be detected at high concentration of ZnO/PI film (>35.1 mol% ZnO) due to the submicron-size ZnO presented in ZnO/PI films which was confirmed by TEM micrograph in figure 5.17. In addition, the films were prepared under argon atmosphere showed the same trend as those prepared under nitrogen atmosphere (Fig F-3). These ZnO/PI films were not as transparent as those Zn nitrate/PI films because submicron-size ZnO hindered the light to pass through the film.

Figure 5.12 showed the effect of ZnO/PI concentration on the light emission intensity and wavelength. The films were imidized at 300°C under nitrogen atmosphere. Adding more ZnO nanoparticles into the films, although the wavelengths of excitation peak of all film were approximately the same (except 117.6 mol% ZnO), the light emission intensity increased and slightly blue shifted from 474 to 458 nm at 3.3 mol% ZnO/PI compared to that of pure PI. Then adding more amounts of ZnO nanoparticles at 35.1 mol% and above, the light emission was not shifted (~1-2 nm) compared to that of 3.3 mol% ZnO/PI. Furthermore, adding only 0.6 mol% of ZnO nanoparticles, the light emission peak at visible wavelength was enhanced by 2.2 times compared to that of pure PI. In addition, the light emission peak of 35.1 mol% of ZnO/PI films enhanced by 7.8 times compared to that of pure PI. Adding more amounts of ZnO nanoparticles at 74.1 and 117.6 mol% ZnO into the films, the light

emission intensity was dramatically decreased which could be due to the self-absorption of ZnO. Fluorescence was generally inversely proportional to concentration which could be attributed to concentration quenching [*25*]. The concentration quenching can be classified into two categories that is, self-quenching and self-absorption. Self-quenching is a collision phenomenon between the molecules in the ground state and those in excited state condition that leads to the energy transfer without fluorescence. Self-absorption is a phenomenon occurring when the wavelength of fluorescence overlaps that of absorption of sample. That leads to the fluorescence which was absorbed by molecules of themselves. This is consistent with the appearance of an increasing absorption in visible region (above 370 nm). Moreover, the visible light emission of all concentrations except 0.6 mol% ZnO nanoparticles in PI films showed two main peaks which were identified at 460 and 485 nm, similar to the result reported by Roy et al [*15*]. The peak at 485 nm could be originated from oxygen vacancy defect in ZnO.

The absorbance and photoluminescence of Zn nitrate/PI film were shown in figure 5.13 and 5.14, respectively. The effect of Zn nitrate/PI films on the absorbance spectrum was shown in figure 5.13. The films were imidized at 300°C under nitrogen atmosphere. The absorption of all concentration showed peaks at 318 nm and absorbed in the range of 300 – 370 nm. The absorption above 370 nm continually increased when Zn nitrate concentration in PI increased which could be due to the increasing in particle size of ZnO in PI films which was confirmed by XRD. However, the exciton absorption peak of all concentration was not shifted compared to that of ZnO/PI films. In addition, the films were prepared under argon atmosphere had the same trends (Fig F-1).

Figure 5.14 showed the effect of ZnO concentration from thermal decomposition of zinc nitrate in PI films on the light emission intensity and wavelength. The films were imidized at 300°C under nitrogen atmosphere. It could be seen that adding only 5 mol% of Zn nitrate in PI film showed highest intensity at visible wavelength compared to other films. In addition, the light emission peak at visible wavelength of 5 mol% of Zn nitrate/PI enhanced by 1.9 times compared to that of the pure PI. On the other hand, the light emission intensity of 10 and 15 mol% Zn nitrate/PI showed lower intensity than that of 5 mol% Zn nitrate/PI.

However, the light emission intensity of 35.1 mol% of Zn nitrate/PI was much lower than that of pure PI. Not only the light emission intensity of 35.1 mol% of Zn nitrate/PI decreased but also that of 74.1 and 117.6 mol% of Zn nitrate/PI continually decreased. It could be due to the aggregation of ZnO nanoparticles. Moreover, the light emission of these hybrid films showed red shifted when compared to that of the pure PI films. It may be attributed to the aggregation of ZnO nanoparticles. However, the light emission of ZnO/PI slightly blue shifted compare to that of pure PI because of no change of ZnO nanoparticle's size in PI films which was confirmed by TEM image (Fig 5.17). This result was confirmed by the appearance of an increasing absorption above 370 nm.

Furthermore, the visible light emission of 5, 10 and 15 mol% Zn nitrate/PI showed two main peaks which could be identified at 486 and 502 nm, similar to the results reported by Roy et al [*15*]. However, all samples emitted green color. Generally, the visible light emission was assumed to be caused by different intrinsic defects in ZnO such as oxygen vacancy and interstitial zinc (450-600 nm) [*26-28*]. The effect of ZnO concentration under argon atmosphere on photoluminescence, which showed the same trend, was shown in appendix F.

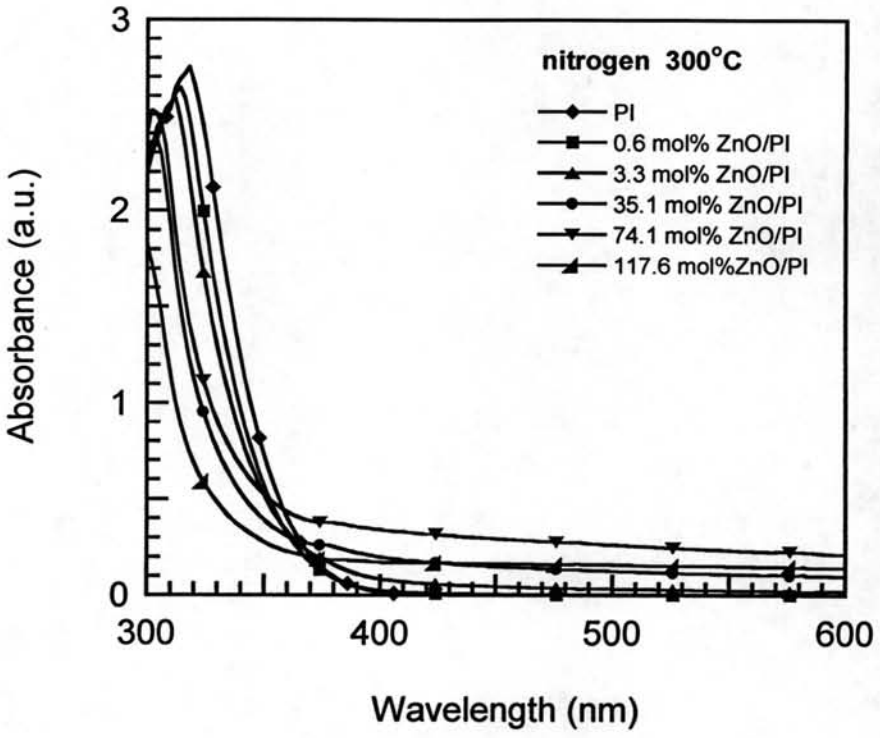

Figure 5.11 Effect of ZnO concentrations on absorbance of ZnO/PI under nitrogen atmosphere at 300°C curing temperature.

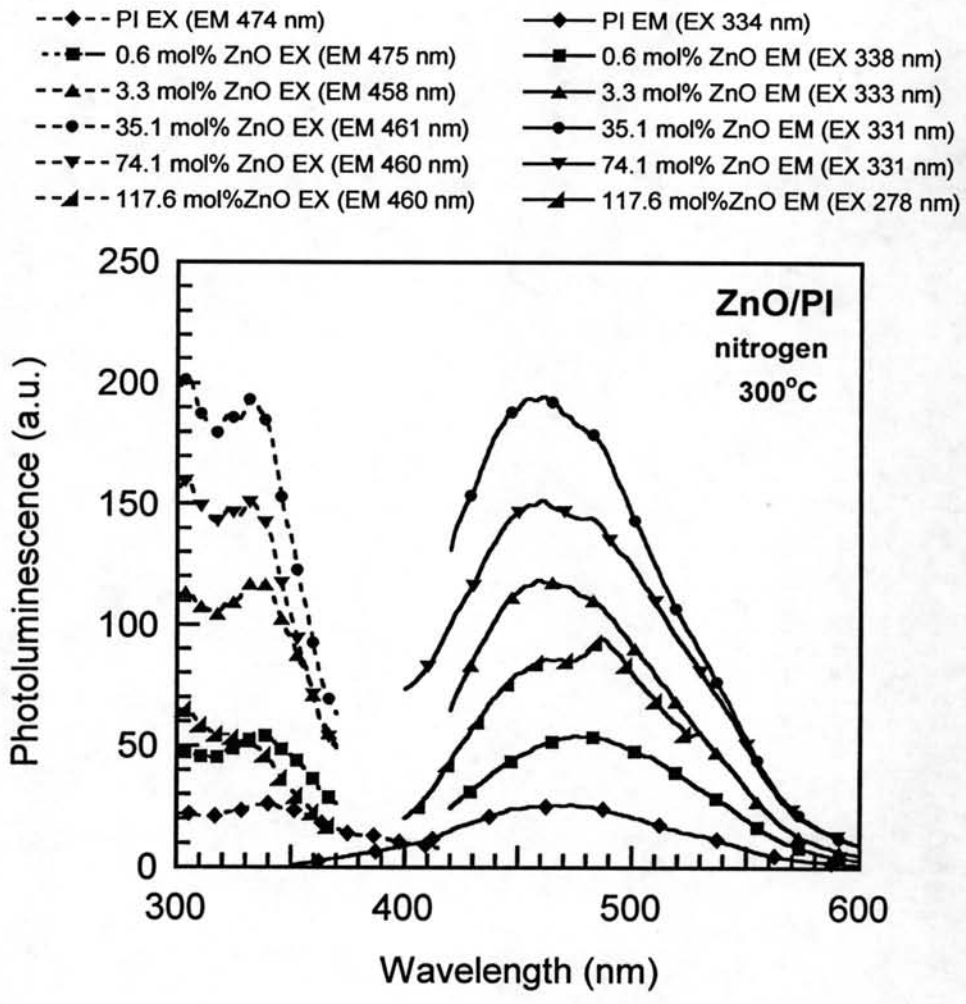

Figure 5.12 Effect of ZnO concentrations on photoluminescence of ZnO/PI under nitrogen atmosphere at 300°C curing temperature.

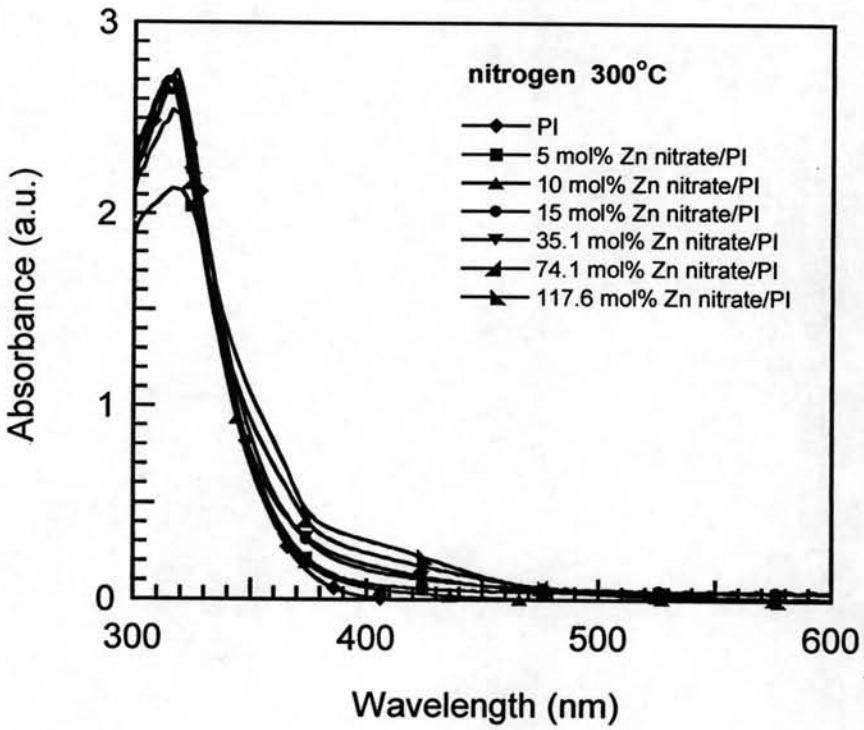

Figure 5.13 Effect of ZnO concentrations on absorbance of Zn nitrate/PI under nitrogen atmosphere at 300°C curing temperature.

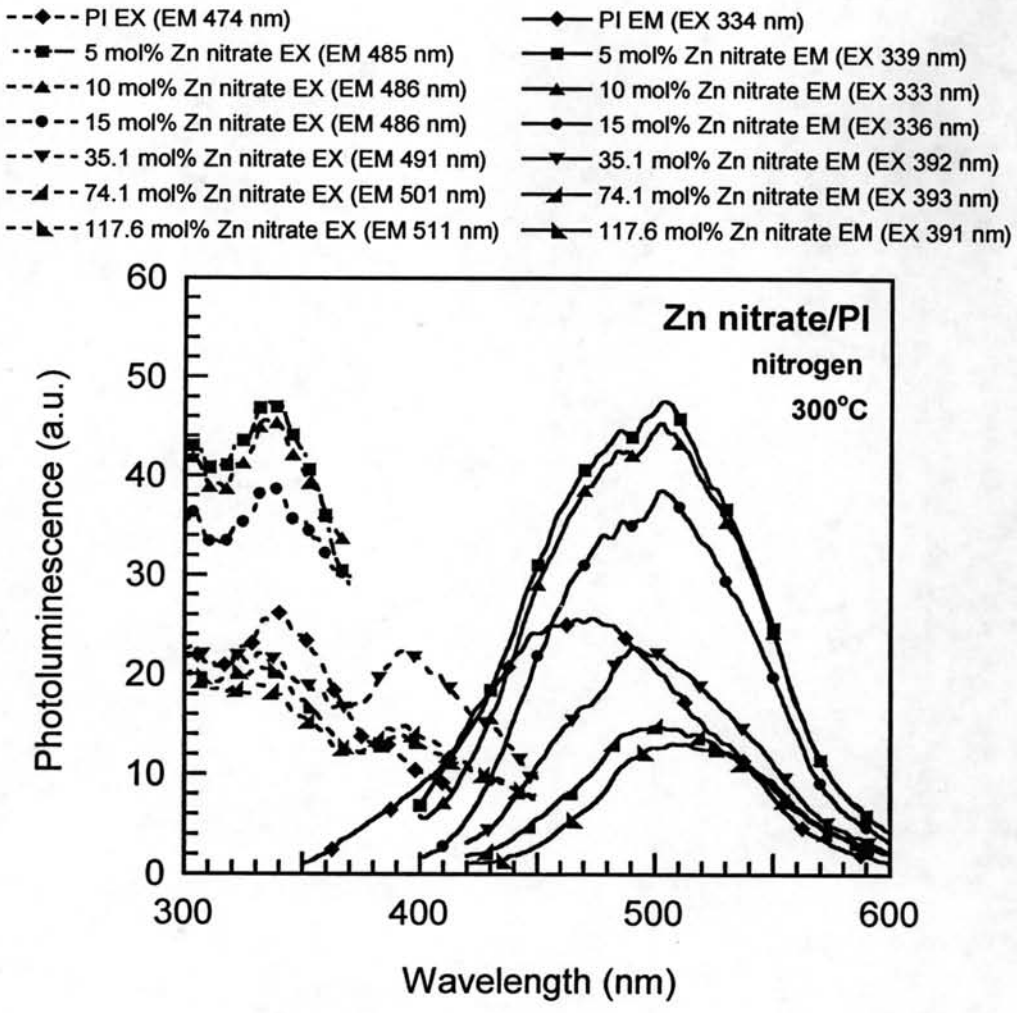

Figure 5.14 Effect of ZnO concentrations on photoluminescence of Zn nitrate/PI under nitrogen atmosphere at 300°C curing temperature.

5.4.4 Effect of the origin of ZnO on photoluminescence

Figure 5.15 showed the effect of the origin of ZnO on absorbance and photoluminescence of PI film at concentration of 35.1 mol%. The films were imidized at 300°C under nitrogen atmosphere. The exciton absorption peak of Zn nitrate/PI at 313 nm and ZnO/PI at 301 nm was observed. The absorption of both PI films in the range of 300-400 nm was observed. However, the increasing of ZnO/PI absorbance (above 400 nm) was observed compared to that of Zn nitrate/PI. Furthermore, the light emission of ZnO/PI showed emission peak at 461 nm, which was blue shifted from 491 nm and much higher intensity than that of Zn nitrate/PI. In addition, the excitation and emission peaks of ZnO/PI were enhanced by 8.7 times when compared to that of Zn nitrate/PI. It could be due to the perfect crystal of ZnO nanoparticles in ZnO/PI films. In the other way, ZnO from thermal decomposition of zinc nitrate caused self-quenching more than ZnO nanoparticles in ZnO/PI films. The effect of ZnO/PI and Zn nitrate/PI on photoluminescence prepared under argon atmosphere showed the same trends at any concentrations as shown in appendix G.

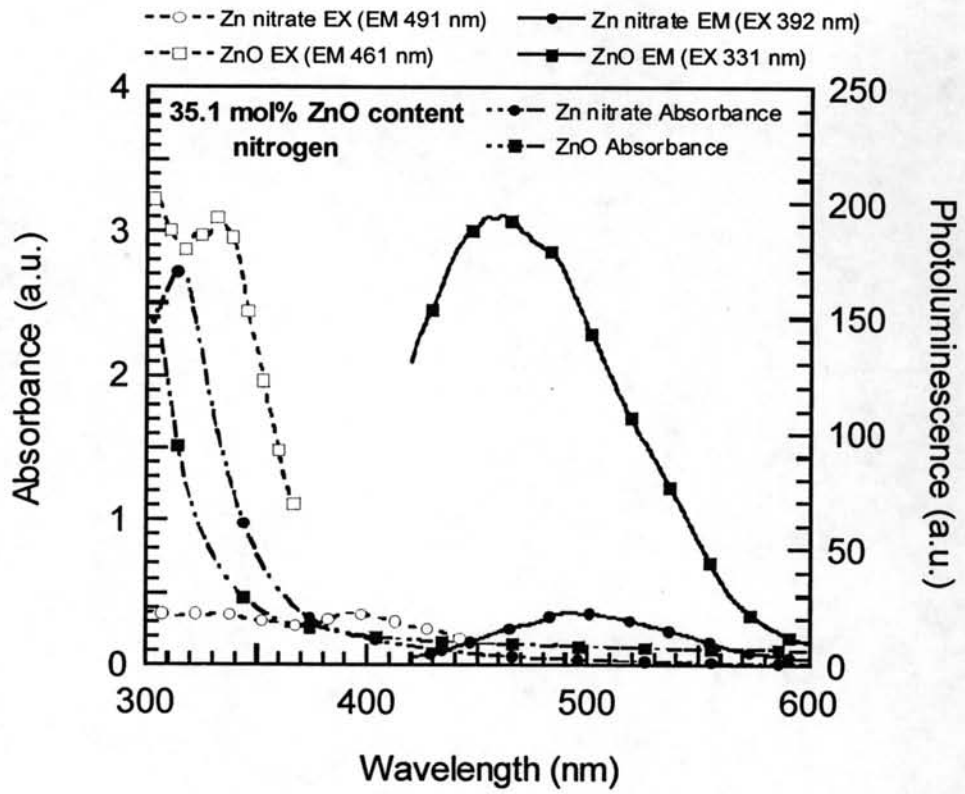

Figure 5.15 Effect of the origin of ZnO at concentration of 35.1 mol% on photoluminescence under nitrogen atmosphere at 300°C curing temperature.

5.5 Dispersion of ZnO nanoparticles in PI films

Transmission electron microscope (TEM) images of 35.1 and 117.6 mol% ZnO/PI films were shown in figure 5.16(a) and (b), respectively. The ZnO nanoparticles were well distributed but poor dispersed in PI films. Furthermore, the aggregation of ZnO nanoparticles with average diameter of 17-90 nm was shown in figure 5.17(a) and (b) and agglomeration of ZnO nanoparticles average size of 114-150 nm was observed. However, the ZnO nanoparticles from thermal decomposition of zinc nitrate can not be observed by TEM image in this study which could be due to the limitation of TEM resolution capacity.

(a)

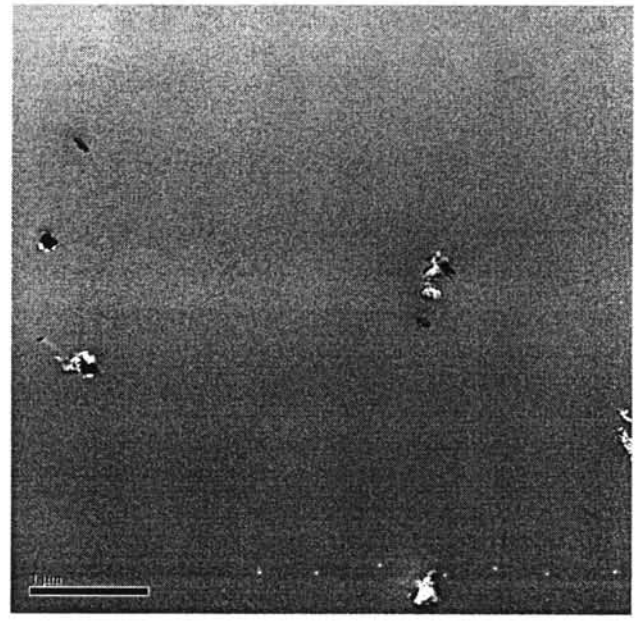

(b)

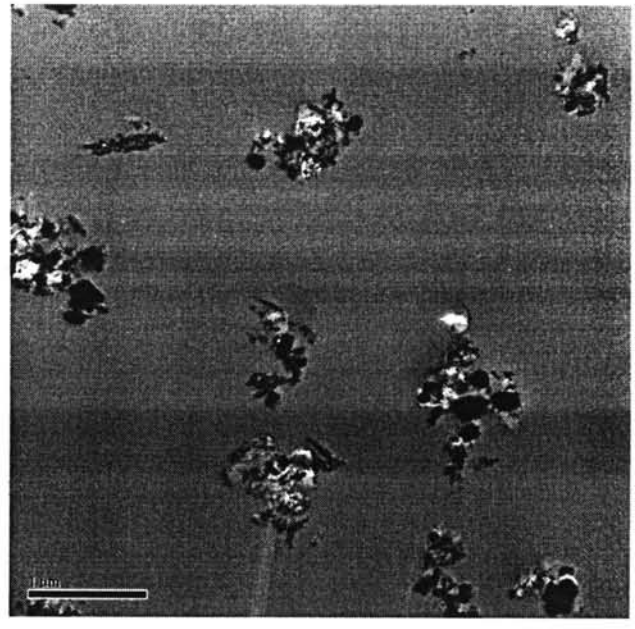

Figure 5.16 TEM image resolution 1 μm of polyimide containing (a) 35.1 mol% ZnO/PI and (b) 117.6 mol% ZnO/PI.

(a)

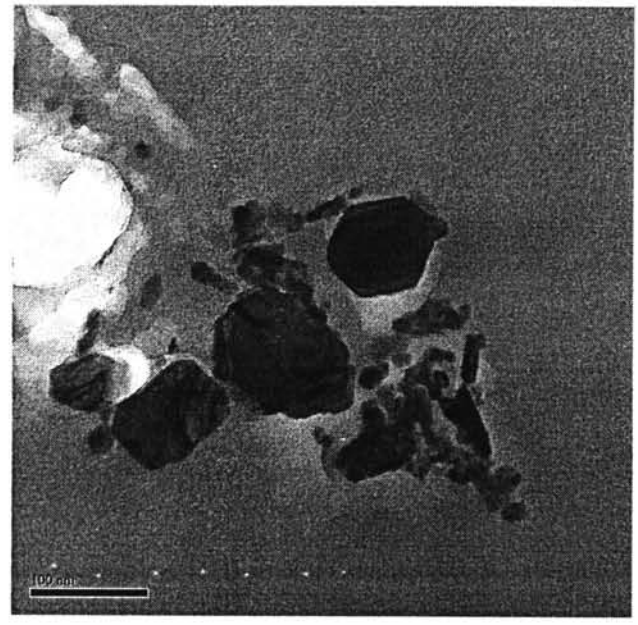

(b)

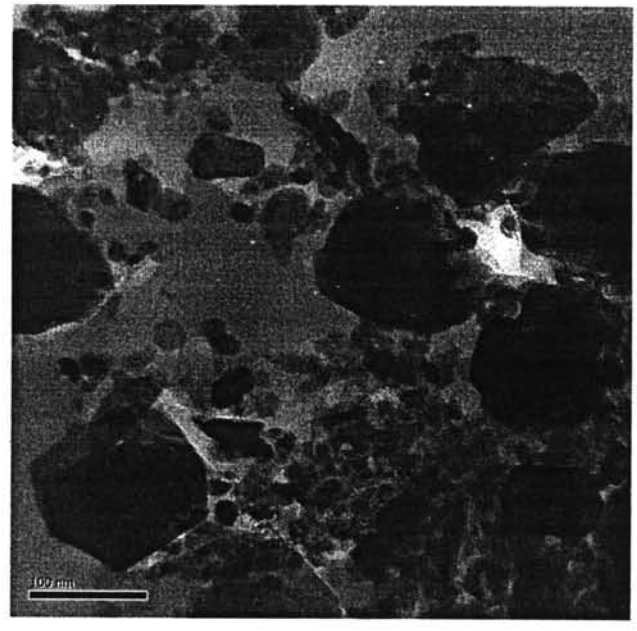

Figure 5.17 TEM image resolution 100 nm of polyimide containing (a) 35.1 mol% ZnO/PI and (b) 117.6 mol% ZnO/PI.